# Thermal-hydrologic mechanism for rainfall-triggered collapse of lava domes

D. Elsworth* ┐
B. Voight ┘ College of Earth and Mineral Sciences, Pennsylvania State University, University Park, Pennsylvania 16802-5000, USA
G. Thompson British Geological Survey, Keyworth, Nottingham NG12 5GG, UK
S.R. Young College of Earth and Mineral Sciences, Pennsylvania State University, University Park, Pennsylvania 16802-5000, USA

## ABSTRACT

**Hazardous gravitational collapses involving hot lava domes can be triggered by intense rainfall, both in periods of active dome growth and volcanic repose. The collapses can evolve into energetic failures involving as much as 90% of the dome, or $>100 \times 10^6$ m$^3$ of dome lava, retrogressively removed over several hours. Understanding such potentially lethal phenomena is vital, but traditional explanations for rain-induced slope failure are problematic for rainfall on hot (typically >400 °C) crystalline lava. In this paper we quantitatively develop a new thermal-hydrologic mechanism that can cause such failures: pressure buildup within fissures due to effusive gas trapped by a rain-saturated dome carapace results in increased destabilizing forces and the loss of mass strength, and ultimately results in failure of the dome. Our mechanistic models are consistent with field observations and provide a quantification of threshold rainfall intensities and durations required to trigger failure.**

**Keywords:** lava dome, rainfall, instability, pyroclastic flows, hazard.

## INTRODUCTION

Gravitational collapses of hot lava domes are extremely hazardous because they can generate explosions and/or lethal pyroclastic flows that reach many kilometers from the source (Newhall and Melson, 1987). Rainfall-induced, pyroclastic-flow–generating collapses have been suggested from a number of volcanoes, such as Mount St. Helens (United States), Merapi (Java), Unzen (Japan), and Montserrat (West Indies) (Mastin, 1994; Yamasato et al., 1998; Voight et al., 2000; Matthews et al., 2002).

Typical among these are the major lava-dome failures on Montserrat on 3 July 1998, 20 March 2000, 29–30 July 2001, and 16–17 July 2003, which directly followed periods of well-documented heavy rainfall (Fig. 1; Norton et al., 2002; Matthews et al., 2002; Herd et al., 2003). These failures contrast with a total of ~26 collapses $>\sim 10^6$ m$^3$, in the period 1995–1999, for which rainfall was not implicated. For these suspected rainfall-related collapses, sustained 2-h-duration intensities as high as 25 mm/h (peak instantaneous rates in bursts to 1 mm/min) and storm totals of 86 mm were recorded and are clearly correlated with seismicity indicating the dome collapse (Matthews et al., 2002) (Fig. 2).

Through the use of the well-documented Montserrat collapses as examples, we consider failure modes for dome collapses and propose a new causative thermal-hydrologic mechanism for such failures. We show that pressure buildup due to effusive gas trapped by a rain-saturated dome carapace results in the loss of mass strength and in increased forces driving instability, and ultimately can trigger lava-dome failure.

## FAILURE MECHANISMS

### Observed Failure Modes

Two failure styles are typified by the Montserrat collapses of 3 July 1998 and 20 March 2000. The earlier event removed a large volume, but limited fraction (~20%), of an immense metastable dome erupted >4 months previously. In contrast, the latter event removed ~90% of a much smaller but newly grown dome (Fig. 1). The 29 July 2001 collapse was similar to 20 March 2000, but double its size (Matthews et al., 2002), and the 13 July 2003 event was more than double that of 29 July 2001 (Herd et al., 2003). The 3 July 1998 event occurred during the period of no dome growth between March 1998 and November 1999 (Norton et al., 2002) and removed ~20% of an oversized lava dome (~$110 \times 10^6$ m$^3$) that had been erupted (and partly eroded) from November 1995 to February 1998. The collapse left a canyon-like slot open to the east (Fig. 1A). In contrast, a smaller dome (~27

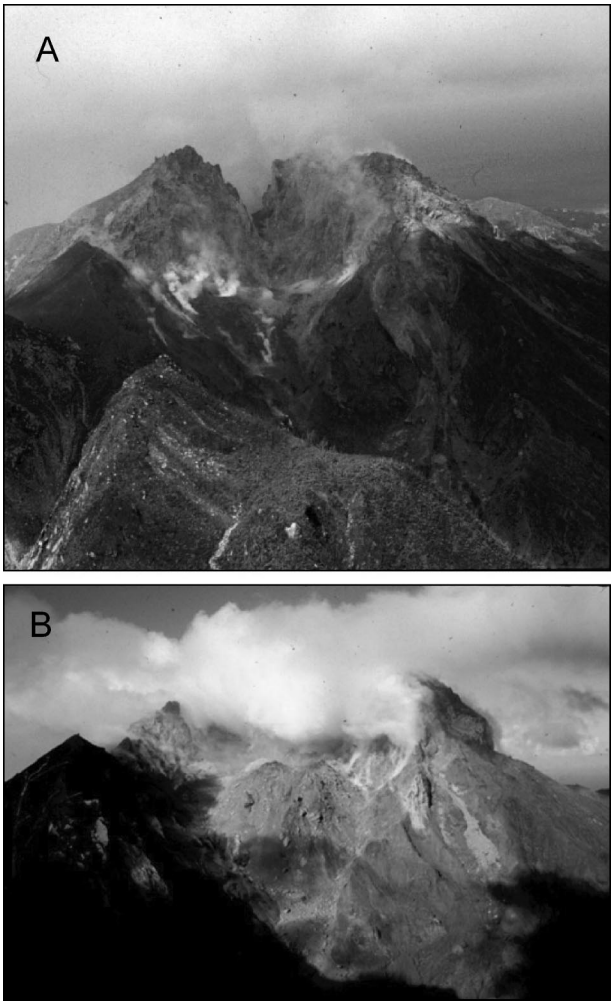


**Figure 1. Soufrière Hills volcano. A: Crater after rain-triggered collapse of lava dome on 3 July 1998, showing resulting collapse scar. B: New lava dome growing in crater in December 1999. Rain triggered collapse of this dome on 20 March 2000; dome was replaced by another lava dome that collapsed on 29–30 July 2001 (see Fig. 2). Crater spans ~1 km at rim.**

*E-mail: elsworth@psu.edu.

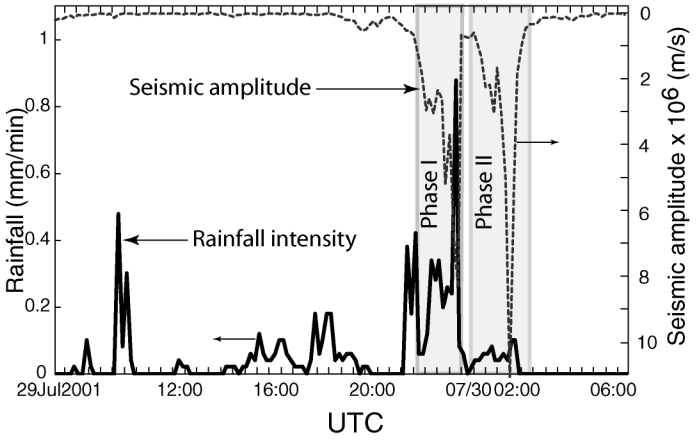


**Figure 2. Correlation of rainfall intensity and seismic amplitude (inverted) for collapse of 29 July 2001. Rainfall intensity recorded by University of East Anglia rain gauges at St. Georges Hill (4 km west of dome) (solid line, read on left axis). Seismic amplitude (short-dashed line, read on right axis) recorded at Windy Hill digital seismic station. Antecedent rainfall began at 0800, in multiple bursts reaching 2 h duration, and may have been important in priming system for failure. Heaviest rainfall was from 2100 UTC (07/29) to midnight (07/30) and ceased at 0230. Dome collapse began at ~2200 and peaked at 1150; second phase of collapse resumed at 0030 and peaked at 0200.**

$\times 10^6$ m$^3$), which had grown ~2.5 m$^3$/s since November 1999 within the enlarged sloping (~15°) scar of this previous failure (Fig. 1B), collapsed on 20 March 2000; ~90% of the dome was removed. In each case, retrogressive collapses were initiated in the latter stages of heavy rainfall, generated a sharp increase in rockfall-type seismicity (Fig. 2), and in some cases were followed by elevated gas flux measurements immediately after the collapse (Norton et al., 2002). The collapses occurred as semicontinuous to sequential failures over periods of several hours. A model is proposed here to explain these observed collapses, for which seismic precursors were largely absent.

### Rainfall-Induced Failure Mechanisms

We consider multiple potential mechanisms that may have contributed to collapse. Conventional mechanisms not involving rain include slope oversteepening (Sparks et al., 2000), gas overpressurization of the dome interior (Voight and Elsworth, 2000; Elsworth and Voight, 2001), and hydrothermal weakening of the dome or its substrate. Storm-triggered destabilization of the steep apron of dome talus has been observed on Montserrat on a number of occasions, e.g., 14 October 2001 (unpublished data from the Montserrat Volcano Observatory), and it is possible that larger failures could then result if unstable, oversteepened lava is thereby exposed. A traditional mechanism for storm-triggered rockslides is rain infilling of joints that elevates destabilizing pore pressures, although such a mechanism is unlikely to work in hot lava because of rapid vaporization of the infiltrating fluid. The extension of surface cracks in lava by rainfall quenching is likely to contribute to failure by the degradation of the mass (fractured rock) strength of the dome materials, although the elevation of interior fluid (gas) pressures appears necessary to generate the scale of failures observed. Consequently, alternative mechanisms are desirable for some of the observed rain-triggered dome-removing failures on Montserrat, with collapse scars that cut deeply into the dome interior (Sparks et al., 2000).

## FAILURE MODEL

We consider the limit equilibrium stability of a dome where the trigger for failure is the augmentation of interior gas pressures, as infiltrating rainwater stanches the escape of magmatic gases through the fractured hot dome carapace (Fig. 3A). The dome becomes less stable

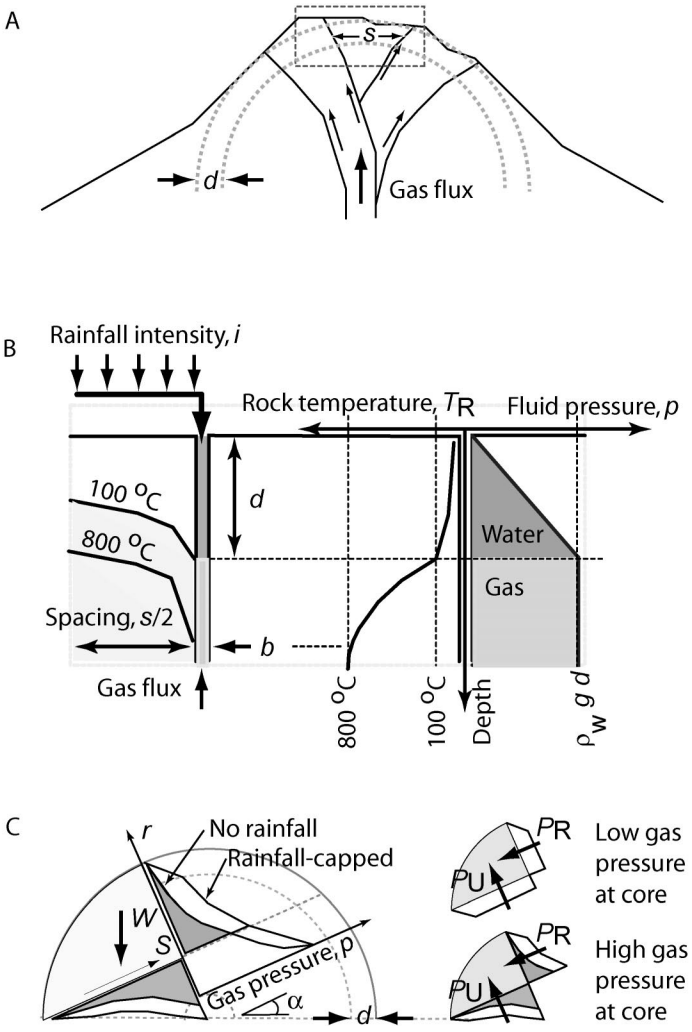


**Figure 3. Schematics of dome geometry, infiltration into carapace, and stability analysis. A: Gas flow in dome is localized on relict shear surfaces (*d* = depth; *s* = fracture spacing). Insets show locations of B and C. B: Infiltrating water penetrates fractures to depth *d*, enabled by locally depressed 100 °C isotherm, and builds water pressure to $p = \rho_w g d$ at infiltration front. C: Existing gas pressures (dark shading) are augmented (unshaded) by stanched gas flow, increasing weakening ($P_U$) and disturbing ($P_R$) fluid forces acting on detached failing dome sector of weight *W*, held by shear resistance, *S*.**

as interior gas pressures build and will ultimately fail if a critical, but undefined, overpressure is reached. Gas overpressure is limited to the static pressure present at the infiltration front within the fractured carapace, defined as the product of penetration depth ($d$) and unit weight ($\rho_w g$) of the infiltrating fluid (Fig. 3B). Consequently, instability may be indexed to the anticipated depth of liquid infiltration, and this depth in turn is limited by the vaporization of the infiltrating fluid.

### Mechanical Instability

We simplify the dome geometry to accommodate the approximate spherical symmetry of gas flow, discharged from a central conduit (Figs. 3A, 3C). The stability of an isolated block on the dome flank is indexed through the ratio of forces resisting downslope movement to those promoting it, as a factor of safety ($F_s$; Voight and Elsworth, 2000). For a degassing vent, gas pressures diminish radially outward from the conduit (Fig. 3C) and apply net uplift ($P_U$) and downslope ($P_R$) forces to the block isolated on a detachment plane inclined at angle $\alpha$ (discussed extensively in Voight and Elsworth, 2000). It is important here to note that capping gas pressures at a peak magnitude of $p = \rho_w g d$ beneath a saturated carapace or occluded fracture to depth

$d$ augments the uplift ($P_U$) and downslope ($P_R$) forces that act additively to destabilize the block (Fig. 3B). This augmentation in pressure (and hence its destabilizing effect) is greatest when gas discharge from the dome core is high (Fig. 3C, lower right inset), but is also present for low fluxes or where vaporization around the liquid infiltration front self-generates overpressure (Fig. 2C, upper right inset). In either case, the limiting pressure at depth $d$ is $p = \rho_w g d$.

**Limits on Interior Gas Pressurization**

The penetration depth of water into the dome is controlled by two factors. First, the carapace must be sufficiently quenched by precipitation to allow the infiltration of rainfall as liquid. Second, carapace fractures must be sufficiently permeable to allow the liquid to penetrate over the limited duration of the rainfall event. The lesser of the two depth predictions will control the height of the resulting water column (Fig. 3B) and therefore the maximum interior gas pressure that may be sealed.

**Thermal limits on liquid penetration.** Although few data exist for important transport parameters in hot dome lavas, sensible ranges may be defined. Near-surface temperatures in the range 800–400 °C are suggested by the periodic detachment and raveling of incandescent blocks of andesite (temperatures in the range 365–640 °C have been measured in pyroclastic flow deposits on Montserrat; Cole et al., 1998). For readers unfamiliar with andesitic dome lavas, we emphasize that the situation for such materials is not comparable to rainfall on, e.g., flowing or ponded basaltic flows (Hardee, 1980), or perhaps rhyolitic obsidian lavas, with an unfractured ductile or fluid interior. On Montserrat the carapace is highly fractured: fractures 10–200 m long have been observed, and large fractures (>50 m deep and of similar spacing) that extend into a highly fissured dome interior have been observed after major collapses (Sparks et al., 2000). These observations confirm the brittle characteristics of gas-rich porphyritic andesite domes, where strength gain is driven primarily by gas exsolution during ascent and extrusion.

The fluid-infiltrated dome carapace is idealized (Fig. 3B, simulating conditions in dashed-line summit box shown in Fig. 3A) as a ubiquitously fractured medium of fracture spacing $s$. Liquid penetration depth $d$ may be estimated by equating the quenching potential (thermal flux) of rainfall discharged from a tributary catchment area into a fracture with the thermal flux conducted across the fracture wall as the penetrating water chills the wall to below boiling. The assumptions of (1) lateral conduction to the fracture and (2) that the catchment surface has been sufficiently chilled by preceding rain events such that the rainfall falling at intensity $i$ over duration $t$ reaches, without evaporation, the fracture, enables the fluid penetration depth $d$ to be defined from a conductive solution (Carslaw and Jaeger, 1958) as

$$d = \frac{\rho_W c_W}{\rho_R c_R} \frac{i s^2}{4\kappa_R} \frac{\Delta T_W}{\Delta T_R} [t_D + \Im(t_D)]. \quad (1)$$

The subscripts R and W represent rock and water, respectively, $\Delta T_W$ represents the change in temperature occasioned by the vaporization of water (i.e., 100 °C minus ~20 °C), $\Delta T_R$ is the quenching of lava-dome rocks at the fracture wall (i.e., ~800 °C minus 100 °C), $\kappa_R$ is thermal diffusivity, $t_D = 4\kappa_R t/s^2$, and

$$\Im(t_D) = \frac{1}{3} - \frac{2}{\pi^2} \sum_{n=1}^{\infty} \frac{(-1)^n}{n^2} e^{-t_D n^2 \pi^2} \cos(n\pi). \quad (2)$$

Hydraulic penetration may be evaluated for initial dome-rock properties of temperature $T_R$ = 400–800 °C, density $\rho_R$ = 2600 kg/m$^3$, heat capacity $c_R$ = 918 J/(kg·K), thermal diffusivity $\kappa_R = 10^{-6}$ m/s$^2$, and standard constants for water at 20 °C (Elsworth, 1989).

For 75 mm of rainfall over 3 h, the resulting hydraulic penetration is smallest for the very narrow spacing of fractures ($s < 0.2$ m), or an equivalent porous medium, where the dome carapace is quenched to a maximum depth of about one-third the storm total rainfall. Above this spacing ($s > 0.2$ m), hydraulic penetration depth $d$ grows linearly with spacing to reach 8 m for fractures spaced 80 m apart in rocks of 800 °C and 20 m penetration for rocks at 400 °C. For fractures spaced only 5 m apart, penetration depths decrease to 0.5 m (800 °C) and 1.4 m (400 °C). The water plugging of the most widely spaced, and most highly gas-conductive, fractures (Fig. 3A) will cause the greatest reduction in gas flow and the largest corresponding increase in trapped overpressures. These highly conductive fractures are the focus of this work.

**Hydraulic limits on liquid penetration.** Where the hydrology is fracture dominated, the parameters of permeability, fluid-displacement pressure (the gas-liquid pressure difference required to overcome interfacial tension and allow liquid to infiltrate the fracture), and secondary porosity may be straightforwardly related. Permeability $k$ may be defined as (Elsworth, 1989)

$$k = \frac{b^2}{12} \frac{b}{s} \quad (3)$$

and linked to fracture porosity $n$ and fracture aperture $b$ as $n = b/s$, to fluid-displacement pressure $p_c$ as

$$p_c \propto \sqrt{n/k}, \quad (4)$$

and to infiltration depth $d$ as $d = it/n$. Measured matrix permeabilities of Montserrat dome rocks are $10^{-12}$–$10^{-14}$ m$^2$ (Melnik and Sparks, 2002) (subboiling hydraulic conductivities of 20–0.2 mm/h) and, for observed fracture spacing >50 m (Sparks et al., 2000), enable bounds to be placed on isothermal infiltration rate and depth penetration. With hydraulic conductivities lower than the sustained rainfall intensities of 25 mm/h, infiltration rate is limited by the saturated permeability of the fractured system. Under the assumptions of a dome permeability of $10^{-12}$ m$^2$ and a fracture spacing of 5 m, 75 mm of rainfall may penetrate, concurrent with the rainfall event, to a depth of 100 m, absent the thermal controls previously discussed.

**Anticipated magnitudes of interior gas overpressures.** Gas overpressures are evaluated for rain infiltration into a representative large, near-dormant dome (July 1998) with nonnegligible (but unmeasured) effusive gas activity (Edmonds et al., 2003) and with a surface that may have been multiply quenched and chilled by previous storms. For an average carapace temperature of 400 °C and permeability of $k = 10^{-12}$ m$^2$, fractures spaced between 5 and 80 m apart may be penetrated, in a given intense storm, to depths of 1.4–21.6 m; these depths represent limits on passive interior gas pressurization to ~20 m of static head (0.2 MPa). For permeabilities $>\sim 10^{-14}$ m$^2$, the role of fluid-displacement pressures is negligible, and the capping pressure magnitude is adequately (and conservatively) represented by the static pressure head at the infiltration front as $p = \rho_w g d$.

## COLLAPSE MODES

On the basis of the prior model and estimates of capped gas overpressures, we examine the predicted styles and timing of collapse of candidate dome geometries, and we contrast these predictions with events observed at Montserrat.

**Evaluated Modes of Collapse**

Idealized collapse modes are examined for simplified dome geometries of large (350 m) and small (200 m) relative heights, for varied inclinations of an assumed detachment plane $\alpha$, and under varied conditions of interior gas pressurization and rainfall capping of the carapace (Fig. 4). Consistent cohesive strengths of ~0.5 MPa and friction angles of 25° are derived from inverse analyses of spine expulsions

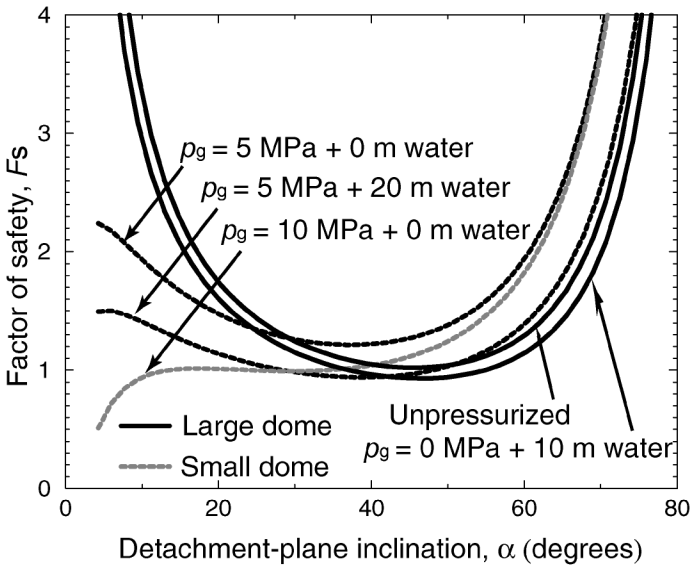


**Figure 4. Variation in factor of safety for small and large domes, subject to applied radially diminishing core pressures (maximum core values of 0, 5, and 10 MPa) and supplemented by uniform gas pressures (0, 10, and 20 m of water head).**

(Sparks et al., 2000; Voight and Elsworth, 2000). For simplicity, a uniform material having these rock-mass parameters is assumed in the analysis, but we recognize that such complexly extruded domes are not actually uniform. Results are similar to those obtained using other reasonable parameter choices.

Absent gas pressurization, a saturated carapace as thick as 50 m exerts a negligible impact on instability (not illustrated). The large dome is metastable when unpressurized; uniform interior pressures corresponding to an infiltration depth of 10 m are adequate to induce failure ($F_s \rightarrow 1$) at an inclination of ~35°–55° (Fig. 4). Such a collapse is roughly comparable to the July 1998 failure that produced, following retrogression, a canyon-like slot in the dome.

For strength parameters consistent with the previously stated values, the unpressurized small dome is stable, but may be brought close to instability by steady core pressures of ~5 MPa (Fig. 4). Pressure augmentation by liquid infiltration to only 20 m (trapped uniform pressures of 0.2 MPa) is sufficient to promote low-angle failure as shallow as 35°–40° and to remove ~20% of the edifice. If interior gas pressures are further augmented at the dome core, e.g., to 10 MPa (Fig. 4), then a failure surface could drive preferentially on a low-angle (~10°–20°), dome-transecting trajectory, potentially capable of piercing the dome core and unroofing the conduit. Although such a failure geometry could roughly simulate the geometry of the March 2000 collapse, 10 MPa overpressure seems excessive for a small dome. We emphasize that ultimately the scar geometry has been controlled by retrogressive failure rather than by the geometry of the initial failures.

### Correlations with Observed Collapses

These proposed mechanistic models broadly reproduce observed timing and geometries of recent rainfall-preceded collapses of the lava dome at Montserrat. The collapse of an oversized and metastable dome (July 1998)—during a period of volcanic repose and absent obvious precursors other than a rainstorm—is consistent with triggering by high-level gas pressurization within the dome. Elevated gas flux measurements immediately after the collapse (Norton et al., 2002) suggest that pressurized gas existed within the dome prior to the collapse, capped by rainfall percolating into the carapace. The near-complete removals of lava domes in March 2000 and July 2001, both in a period of reinitiated effusive activity and absent other precursors, are consistent with gas pressurization of the dome core, critically augmented by the partial sealing of the dome carapace. In each case, collapse geometry and timing are reasonably consistent with available geometric, transport, and strength parameters used in modeling, although it should be appreciated that the collapses are also influenced strongly by retrogressive failure processes that ensue once the key blocks have failed.

Understanding the complex mechanisms of rainfall-triggered instability is important because such failures can occur without warning from standard solid-earth precursory signatures and yet may generate extremely hazardous, large-volume, gas-charged dome-collapse pyroclastic flows and surges. Such correlations emphasize the need to include rainfall monitoring with traditional volcano monitoring methods in order to aid the anticipation of hazardous collapses.


### ACKNOWLEDGMENTS

This work is a result of partial support from National Science Foundation grants CMS-9908590, EAR-9909673, and EAR-0116826. The generous support of colleagues at the Montserrat Volcano Observatory (MVO) is acknowledged, and we thank A. Matthews, University of East Anglia, for permission to use rain-gauge data. Comments on early ideas by scientists at MVO and at Cascade Volcano Observatory are appreciated, as are helpful reviews of the manuscript by S. Anderson, T. Druitt, G. Mattioli, and C. Newhall.


### REFERENCES CITED


Carslaw, H.S., and Jaeger, J.C., 1958, Conduction of heat in solids: Oxford, Oxford University Press, 510 p.

Cole, P.D., Calder, E.S., Druitt, T.H., Hoblitt, R., Robertson, R., Sparks, R.S.J., and Young, S.R., 1998, Pyroclastic flows generated by gravitational instability of the 1996–1997 lava dome of Soufrière Hills volcano, Montserrat: Geophysical Research Letters, v. 25, p. 3425–3428.

Edmonds, M., Pyle, D.M., Oppenheimer, C.M., and Herd, R.A., 2003, $SO_2$ emissions 1995–2001 from Soufriere Hills volcano, Montserrat WI and their relationship to conduit permeability, hydrothermal interaction and degassing regime: Journal of Volcanology and Geothermal Research, v. 124, p. 23–43.

Elsworth, D., 1989, Thermal permeability enhancement of blocky rocks: Plane and radial flow: International Journal of Rock Mechanics, v. 26, p. 329–339.

Elsworth, D., and Voight, B., 2001, The mechanics of harmonic gas-pressurization and failure of lava domes: Geophysical Journal International, v. 145, p. 187–198.

Hardee, H.C., 1980, Solidification in Kilauea Iki lava lake: Journal of Volcanology and Geothermal Research, v. 7, p. 211–233.

Herd, R., Edmonds, M., Strutt, M., and Ottermeiler, L., 2003, The collapse of the lava dome at Soufriere Hills volcano, 12–15 July 2003: Eos (Transactions, American Geophysical Union), v. 84, no. 46, p. F1596.

Mastin, L., 1994, Explosive tephra emissions at Mount St. Helens, 1989–1991—The violent escape of magmatic gas following storms: Geological Society of America Bulletin, v. 106, p. 175–185.

Matthews, A., Barclay, J., Carn, S., Thompson, G., Alexander, J., Herd, R., and Williams, C., 2002, Rainfall-induced volcanic activity on Montserrat: Geophysical Research Letters, v. 29, no. 13, 1644, doi: 10.1029/2002GL014863.

Melnik, O., and Sparks, R.S.J., 2002, Dynamics of magma ascent and lava extrusion at Soufriere Hills volcano, Montserrat, *in* Druitt, T.H., and Kokelaar, B.P., eds., The eruption of Soufriere Hills volcano, Montserrat, from 1995 to 1999: Geological Society [London] Memoir 21, p. 153–172.

Newhall, C.G., and Melson, W.G., 1987, Explosive activity associated with growth of volcanic domes: Journal of Volcanology and Geothermal Research, v. 17, p. 111–131.

Norton, G.E., Watts, R.B., Voight, B., Mattioli, G.S., Herd, R.A., Young, S.R., Devine, J.D., Aspinall, W.P., Bonadonna, C., Baptie, B.J., Edmonds, M., Harford, C.L., Jolly, A.D., Loughlin, S.C., Luckett, R., and Sparks, R.S.J., 2002, Pyroclastic flow and explosive activity of the lava dome of Soufriere Hills volcano, Montserrat, during a period of virtually no magma extrusion, *in* Druitt, T.H., and Kokelaar, B.P., eds., The eruption of Soufriere Hills volcano, Montserrat, from 1995 to 1999: Geological Society [London] Memoir 21, p. 467–482.

Sparks, R.S.J., Murphy, M.D., Lejeune, A.M., Watts, R.B., Barclay, J., and Young, S.R., 2000, Control on the emplacement of the andesite lava dome of the Soufriere Hills volcano, Montserrat by degassing-induced crystallization: Terra Nova, v. 12, p. 14–20.

Voight, B., and Elsworth, D., 2000, Instability and collapse of lava domes: Geophysical Research Letters, v. 27, p. 1–4.

Voight, B., Constantine, E., Siswowidjoyo, S., and Torley, R., 2000, Historical eruptions of Merapi volcano, central Java, Indonesia, 1768–1998: Journal of Volcanology and Geothermal Research, v. 100, p. 69–138.

Yamasato, H., Kitagawa, S., and Komiya, M., 1998, Effect of rainfall on dacitic lava dome collapse at Unzen volcano, Japan: Papers in Meteorology and Geophysics, v. 48, no. 3, p. 73–78.



Manuscript received 8 April 2004
Revised manuscript received 9 July 2004
Manuscript accepted 10 July 2004

Printed in USA